Experimental Surface Pressures on Cone-Derived Waveriders for $M_\infty = 3$-5

M.C. Jischke* and M.L. Rasmussen†
The University of Oklahoma, Norman, Oklahoma
and
D.C. Daniel‡
Air Force Armament Laboratory, Eglin Air Force Base, Florida

Surface pressure data are presented for two waverider lifting-body configurations in the Mach number range of 3-5 and unit Reynolds number of 2×10^6/ft. Angle of attack and sideslip angle were varied in the range ± 20 deg. Comparison data are also given for an elliptic cone with a 1.87 major/minor axis ratio. The data complement earlier results for forces and moments. Present results corroborate the basic conical flow assumption and the first-order perturbation theory that underlie the waverider configuration design. Off-design data show smooth variations from the design conditions with no evidence of strong secondary shocks or deviations from ideal conical flow.

Nomenclature

C_p = pressure coefficient
e = eccentricity
K_δ = hypersonic similarity parameter, $M_\infty \delta$
M_∞ = freestream Mach number
p = pressure
V_∞ = freestream velocity
α = angle of attack
β = angle of sideslip
δ = semivertex angle of basic cone
ϵ = eccentricity parameter
θ = polar angle
θ_m = see Eq. (6)
θ_s = shock angle
ρ_∞ = freestream density
ϕ = azimuthal angle

Introduction

THE maneuverability requirements for future missiles in the high-supersonic, low-hypersonic Mach number range emphasize high-lift, log-drag configurations with good control effectiveness. These requirements lead to consideration of noncircular airframes that efficiently integrate volumetric storage, lifting capability, and propulsion components such that aerodynamic heating and radar detectability are minimized and lift-to-drag ratios are maximized. Giragosian,[1] Fleeman,[2] and Nielsen[3] discuss these requirements in some detail.

A comprehensive research program is being conducted to study the aerodynamics of lifting-body configurations operating in the Mach number range of interest. Much of the theoretical analysis is based on small perturbations of axisymmetric flows past circular cones; the perturbations resulting from small angles of attack[4] and/or small deviations of the cone cross section from a circle.[5,6] By this means, accurate approximate analytical results are obtained for shock shapes and shock-layer structures. Since any streamsurface can be utilized as a solid surface in an inviscid flow, lifting-body configurations can be constructed when freestream (or other) upper surfaces are selected to complement the lower conical-flow streamsurfaces. These resulting aerodynamic shapes are called cone-derived waveriders because they appear to ride on a conical shock wave attached beneath them. The generation of these shapes and properties of their known shock-layer structure are discussed by Rasmussen.[7]

Rasmussen, et al.[8] have presented six-component force and moment data for two cone-derived waveriders in the Mach number range of 3-5. Comparison data were also presented for an elliptic cone with a 1.87 major-to-minor axis ratio. In addition, schlieren data for the waverider shock-wave positions were presented together with results of surface oil-flow studies. Maximum lift-to-drag ratios of the waveriders were found to be 2.5 times greater than that of the comparative elliptic cone.Normal-force and rolling-moment coefficients, along with the lift-to-drag ratio, were found to decrease for the waveriders as M_∞ increased. The force and moment data substantiated the accuracy of the perturbation theory of Rasmussen[7] for the on-design conditions and showed the deviations resulting from changes in orientation and Mach number. The schlieren data together with the oil-flow studies suggested that the flows were conical and clean, without strong secondary shocks or interruptions, over the entire range of testing conditions. These results, when taken with the supporting theoretical background, make the cone-derived waveriders very attractive and viable contenders for future hypersonic missile and aircraft configurations.

In this paper, we extend the results of Rasmussen et al.[8] by presenting complementary experimental results for surface pressure on the two waverider configurations and the elliptic cone. The new results will be presented in the form of a pressure coefficient C_P defined as

$$C_P = \frac{p - p_\infty}{\frac{1}{2}\rho_\infty V_\infty^2} \tag{1}$$

Presented as Paper 82-0249 at the AIAA 20th Aerospace Sciences Meeting, Orlando, Fla., Jan. 11-14, 1982; submitted Jan. 14, 1983; revision received July 11, 1983.

*Dean, College of Engineering. Associate Fellow AIAA.
†Professor, Aerospace, Mechanical and Nuclear Engineering. Associate Fellow AIAA.
‡Research Manager. Associate Fellow AIAA.

as a function of position for a variation of ±20 deg in angle of attack and sideslip over the Mach number range of 3-5.

Pike[9] has presented surface pressure distributions on waveriders derived from circular cones at zero angle of attack. The measured surface pressures agreed quite well with theory at the design conditions. The effects of leading-edge rounding were shown to be important only close to the leading edge. Although the waverider bodies investigated by Pike were derived from axisymmetric conical flows, the bodies themselves were not conical. The waverider configurations in the present investigation, derived from nonaxisymmetric conical flow, are cones themselves. Thus, the surface pressures should be constant along rays from the vertex, even under off-design conditions.

Description of Models

Sketches of model configurations tested are given in Fig. 1. All of the models were constructed of stainless steel and had the same length, $L=60$ cm (23.62 in.), measured along the basic-cone axis from which they were derived. The other dimensions are indicated in Fig. 1 and given in Table 1, along with the base area A_b. The position of the body-fixed coordinate system is shown also. The jagged curves in Fig. 1 indicate the theoretical position of the shock wave at the design conditions, $M_\infty=4$.

The model shown in Fig. 1a was derived from the flow past a circular cone at angle of attack, as described by Rasmussen[7]; referred to in this paper as the circular-cone waverider. The flow in the shock layer is the same as the flow on the leeward side of an inclined circular cone. The shape of the curved surface, which is a conical streamsurface in the inclined-cone flow, has been approximated by the method of analysis of Rasmussen,[7] and is given in spherical coordinates by

$$\frac{\theta}{\delta}=1+0.34\left[\tan\left(\frac{\pi}{2}-\frac{\phi}{2}\right)\right]^{12.5} \tag{2}$$

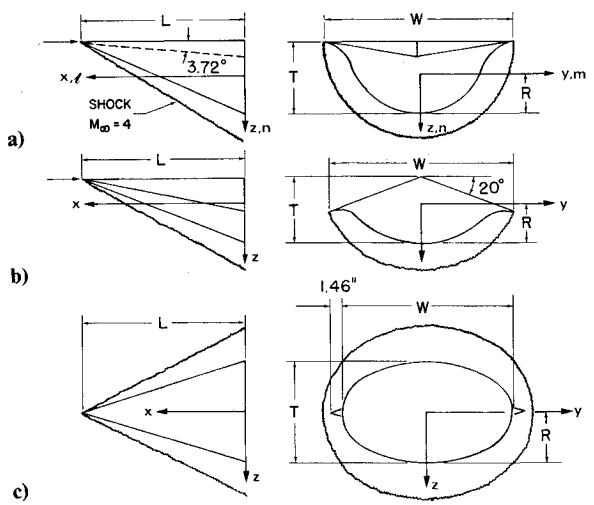

Fig. 1 Model configurations: a) circular-cone waverider, b) elliptic-cone waverider, c) elliptic cone with winglets.

Table 1 Model dimensions (cm.)

	L	W	T	R	A_b cm.^{2}
Circular-cone waverider	60.0	55.8	20.2	11.3	668
Elliptic-cone waverider	60.2	54.6	18.1	11.7	489
Elliptic cone	60.0	57.6	30.9	15.4	1397

where θ is the polar angle measured from the basic-cone axis (parallel to the x axis but passing through the vertex), and ϕ is the azimuthal angle measured around the basic-cone axis such that $\phi=\pi$ is in the z direction. The semivertex angle of the basic cone is denoted by δ, which for this model is $\delta=18.62$ deg. The angle of attack defining this waverider configuration was selected as $\alpha/\delta=0.2$, or $\alpha=-3.72$ deg, which determines the angle between the basic-cone axis and the symmetry ray of the upper surface.

The model shown in Fig. 1b was derived from the flow past an elliptic cone at zero angle of attack and is referred to as the elliptic-cone waverider. The shape of the curved surface, which is a conical streamsurface for the elliptic-cone flow, is given approximately by

$$\frac{\theta}{\delta}=1-0.1\cos2\phi+\left(0.39+0.1\cos2\phi\right)\left[\frac{\tan(\pi-\phi)}{2.75}\right]^{7.69} \tag{3}$$

The basic-cone angle for this model was also selected as $\delta=18.62$ deg. The eccentricity parameter ϵ as defined in the Fourier series representation of Ref. 5 was selected such that $\epsilon/\delta=0.1$.

The design Mach number for these waverider models is $M_\infty=4$. Thus, the pertinent hypersonic similarity parameter is $K_\delta=M_\infty\delta=1.3$. This value of K_δ was used to determine the numerical factors in Eqs. (2) and (3). According to Rasmussen,[7] the circular-cone waverider is said to have positive dihedral and the elliptic-cone waverider is said to have negative dihedral.

For the design condition, the theoretical shock shape for the circular-cone waverider is

$$\theta_S/\delta=1.34-0.04\cos\phi \tag{4}$$

and for the elliptic-cone waverider the shock shape is

$$\theta_S/\delta=1.34-0.06\cos2\phi \tag{5}$$

These shocks are attached to the waverider lips at $\phi=90$ deg for the circular-cone waverider model and at $\phi=110$ deg for the elliptic-cone waverider model.

Figure 1c shows the elliptic-cone model. The equation for the elliptic cone in spherical coordinates is

$$\tan\theta=\tan\theta_m/\sqrt{1+e\cos2\phi} \tag{6}$$

with $\theta_m=17.79$ deg and $e=0.5534$. These values correspond to a major/minor axis ratio of 1.87. According to the perturbation analysis of Rasmussen,[5,7] the corresponding basic cone angle is 18.68 deg, which is nearly the same as that for the two waverider models. Thus, the pertinent hypersonic similarity parameter is about $K_\delta=1.3$ for $M_\infty=4$. The perturbation analysis of Ref. 5 yields an eccentricity factor of $\epsilon/\delta=0.478$. This elliptic cone is thus much more eccentric than the elliptic cone from which the elliptic-cone waverider was derived.

Experimental Conditions

The tests were run in wind tunnel A of the Von Karman Facility at the USAF Arnold Engineering Development Center. Tunnel A is a continuous-flow, closed-return, variable-density wind tunnel with an automatically driven flexible-wall nozzle and 40×40 in. test section. The tunnel is equipped with a model injection system which allows removal of the model from the test section while the tunnel remains in operation. A complete description of the tunnel and airflow calibration information is given in Ref. 10.

The experiments were conducted at Mach numbers of 3.0, 3.5, 4.0, 4.5, and 5.0. On-design conditions for the waveriders were at $M_\infty=4.0$ and $\alpha=-3.72$ deg for the circular-cone waverider, and $\alpha=0$ for the elliptic-cone waverider, both with

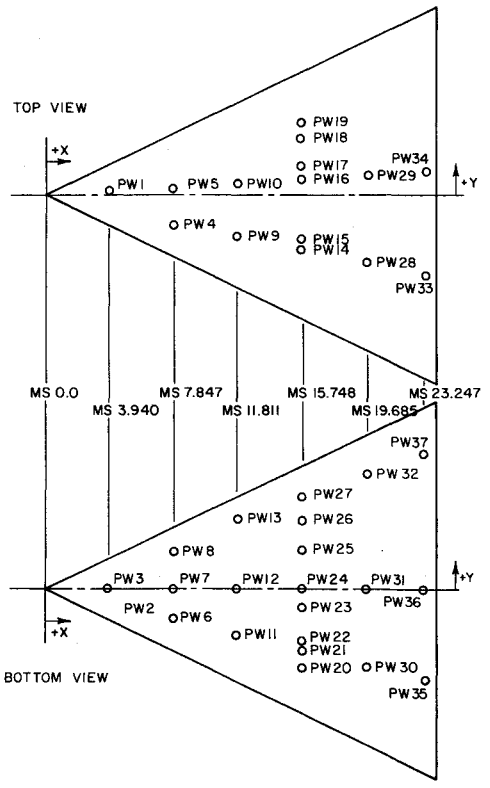

Fig. 2a Pressure orifice location and designation (circular-cone waverider).

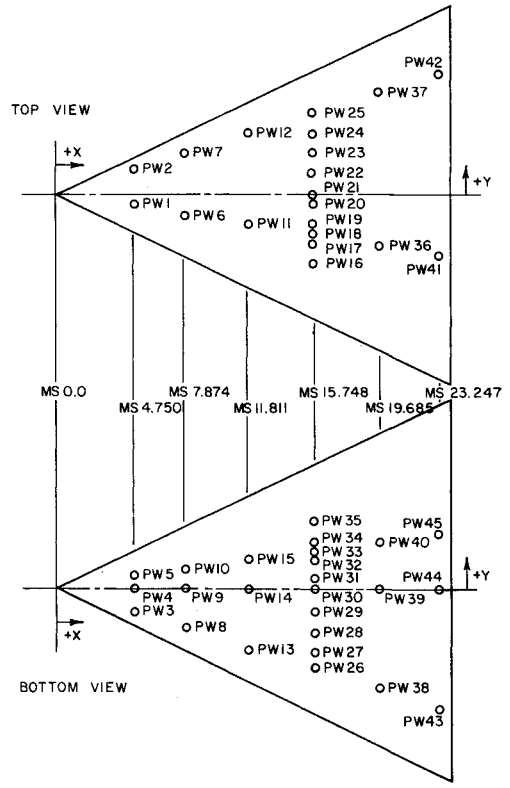

Fig. 2b Pressure orifice location and designation (elliptic-cone waverider).

zero sideslip. All other conditions were off-design conditions. The initial tests recorded six components of force and moment data and visual schlieren and oil-flow data. These results were reported in Ref. 8. Surface pressure data were then recorded at 45 surface positions on the models as indicated in Fig. 2 where the various surface pressure ports are numbered.

The nominal unit Reynolds number for the tests was 2×10^6/ft. Data were taken for the Mach numbers cited previously. A complete summary of the test conditions is given in Ref. 10.

Surface Pressures

The surface pressure data will be presented in three parts. First, data will be given to confirm the underlying conical flow assumption. Second, on-design results will be presented that will verify the first-order perturbation theory upon which the waverider model designs are based. Third, data will be given to illustrate the off-design behavior that arises as a consequence of changes in model orientation and Mach number. Comparative data for the elliptic cone will be presented also.

Conical Flow Assumption

Flows are said to be conical if the physical conditions, such as pressure and velocity, do not vary with position along any ray through an origin (referred to as the vertex). A conical body is obtained as the surface generated by a straight line, one point of which is held fixed and another point of which is made to traverse a closed path. (The fixed point is the apex of the body.) The two waveriders and the elliptic cone models are examples of conical bodies.

An otherwise uniform supersonic flow past a conical body generates a conical flowfield provided the body is sufficiently slender. The analysis from which the waverider configurations are developed is predicated upon the conical-flow assumption.

Figures 3a and 3b show surface-pressure data for the two waverider models at $M_\infty = 4$ and various angles of attack, including the design condition. Similar data were obtained for the elliptic-cone model. The data are presented in the form of a surface pressure coefficient at various positions along different rays through the vertex of the models. These data, as well as other data not given here, show that there is no significant variation of the surface pressure along a ray through the vertex and thus confirm the conical-flow assumption. In addition, these data establish that the flow remains conical over the entire range of conditions examined, including both design and off-design conditions. Thus, the conical flow assumption is well founded.

On-Design Conditions

Figure 4 compares the measured surface pressure coefficient as a function of position at $M_\infty = 4$ with the theoretical results obtained using the first-order perturbation theory of Rasmussen.[5,7] Recall that the waverider models are on their design conditions at $M_\infty = 4$. Figure 4a gives the comparison for the circular-cone waverider which is at the design condition at an angle of attack $\alpha = -3.72$ deg. Figure 4b gives the same comparison for the elliptic-cone waverider which is at the design condition at zero angle of attack. The theoretical results are calculated from the first-order perturbation theory of Rasmussen[5,7]

$$\frac{C_p}{\delta^2} = \frac{c_{p_0}}{\delta^2} + \frac{\alpha}{\delta}\frac{C_{p_0}}{\delta}\cos\phi + \frac{\epsilon}{\delta}\frac{C_{p_2}}{\delta}\cos 2\phi \qquad (7)$$

Here, c_{p_0}/δ^2, C_{p_0}/δ, and C_{p_2}/δ are known functions of the hypersonic small-disturbance parameter K_δ and the ratio of specific heats γ.

The results in Fig. 4 show an almost remarkable agreement between theory and experiment for the on-design condition. These results show that the first-order perturbation theory is quite accurate and lends confidence to the analytical methods by which the waveriders are designed.

Figure 5 compares the measured surface pressure coefficient on the elliptic cone at $M_\infty = 4$ for a range of angles of attack with those computed from the first-order perturbation theory. Here, $\delta = 18.68$ deg and thus $K_\delta = 1.3$. The eccentricity

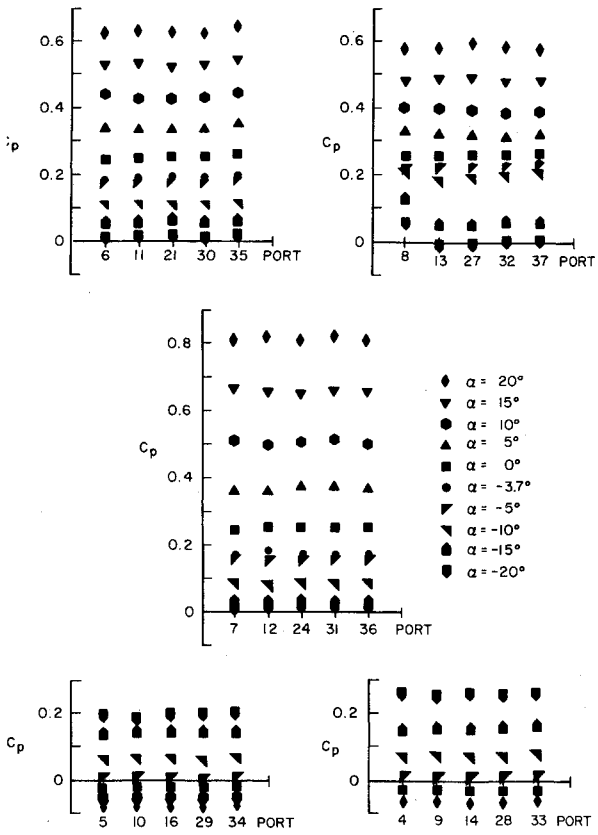

Fig. 3a Measured surface pressure coefficient along rays through the circular-cone waverider vertex ($M_\infty = 4$, $\beta = 0$, $\delta = 0.326$).

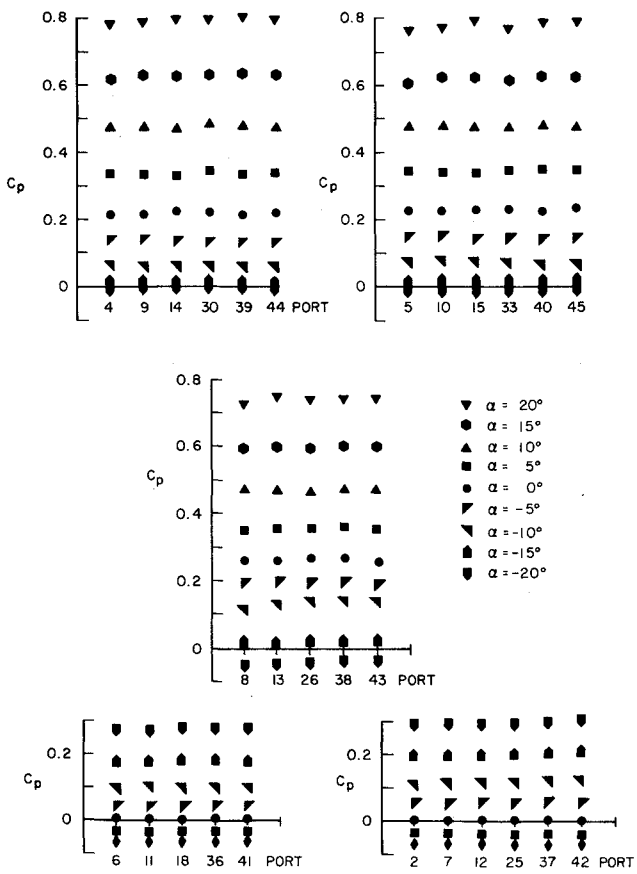

Fig. 3b Measured surface pressure coefficient along rays through the elliptic-cone waverider vertex ($M_\infty = 4$, $\alpha = 0$, $\delta = 0.326$, $\epsilon_2 = 0.0326$).

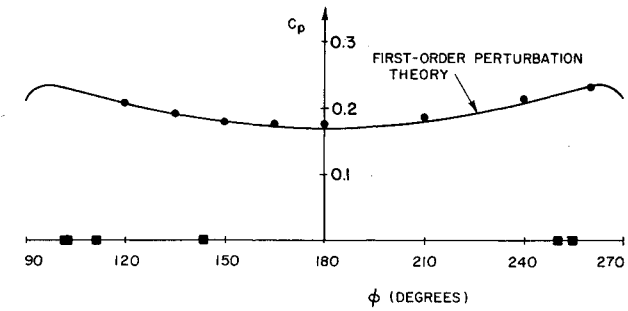

Fig. 4a Comparison of theory and experiment for circular-cone waverider surface pressure coefficient ($M_\infty = 4.02$, $\alpha = -3.70$ deg, $\beta = 0$).

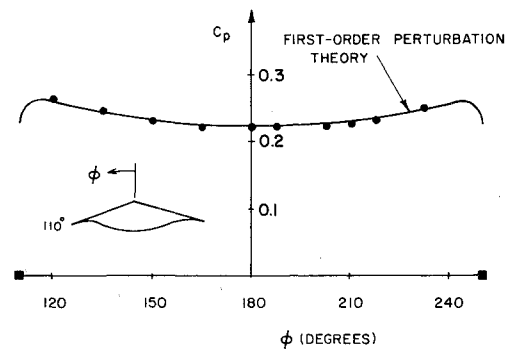

Fig. 4b Comparison of theory and experiment for elliptic-cone waverider surface pressure coefficient ($M_\infty = 4.02$, $\alpha = \beta = 0$).

factor $\epsilon/\delta = 0.478$; a value sufficiently large that the perturbation theory is likely to yield significant errors, as shown in the comparison in Fig. 5. Thus, the first-order perturbation theory can be used in designing waverider configurations only if α/δ and ϵ/δ are sufficiently small compared to unity.

Off-Design Conditions

Figure 6 presents off-design surface pressure coefficient data for the circular-cone waverider for a freestream Mach number of 4. These data were taken at model station 15.748 (see Fig. 2), although they are valid for any downstream location with the same azimuthal angle ϕ because of the conical flow condition. Data for $M_\infty = 3.0$, 3.5, 4.5, and 5.0, not presented here, do not show any important differences from the data presented herein. The data for all five Mach numbers are available in tabular form in Ref. 10 and in graphical form in Ref. 13. Figure 6a gives compression surface data for angles of attack from -20 to $+20$ deg at zero sideslip angle. Figure 6b gives the corresponding upper surface data. Results for sideslip angles from 0 to -20 deg at zero angle of attack are presented in Fig. 6c for the compression surface, while Fig. 6d gives the corresponding upper surface results. In all of these figures the actual data points are plotted as solid symbols. In order to be able to connect the data points with solid lines in a fashion that would preserve the symmetry in the zero sideslip cases, these data points were reflected about $\phi = 180$ deg to give the open data points in Figs. 6 and 7. Thus, the open data points in these figures do represent actual measurements; they are obtained by assuming symmetry at about $\phi = 180$ deg. Examination of these data and those not shown indicates that Mach number variation from 3 to 5 has little effect on the pressure-coefficient distribution, although the maximum pressure coefficient does decrease as M_∞ increases. Also, these data do not show evidence of strong secondary shock waves for off-design conditions, although a compression region does appear in the center region of the upper surface at positive angles of attack. As theoretical calculations for the off-design behavior

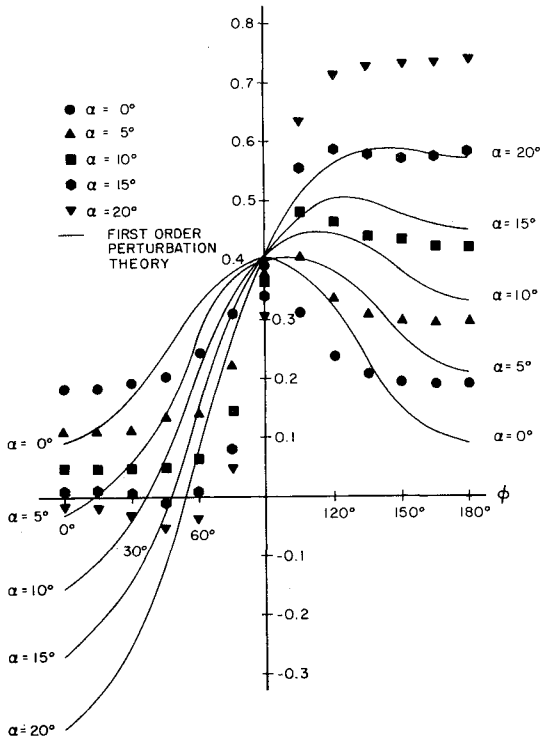

Fig. 5 Surface pressure coefficient on elliptic cone, comparison of perturbation theory and experiment ($M_\infty = 4$, $\beta = 0$, $\delta = 0.326$, $\epsilon = 0.156$).

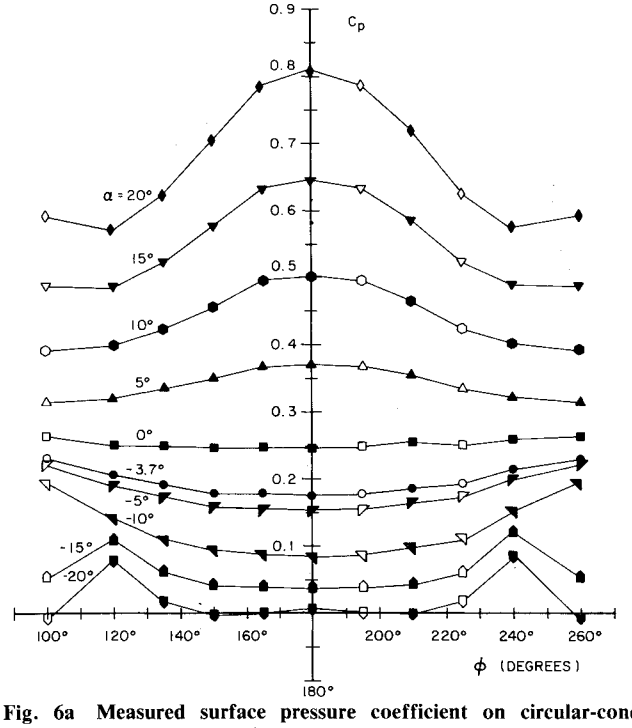

Fig. 6a Measured surface pressure coefficient on circular-cone waverider lower compression surface at various angles of attack ($M_\infty = 4$, $\beta = 0$, open symbols obtained by symmetry).

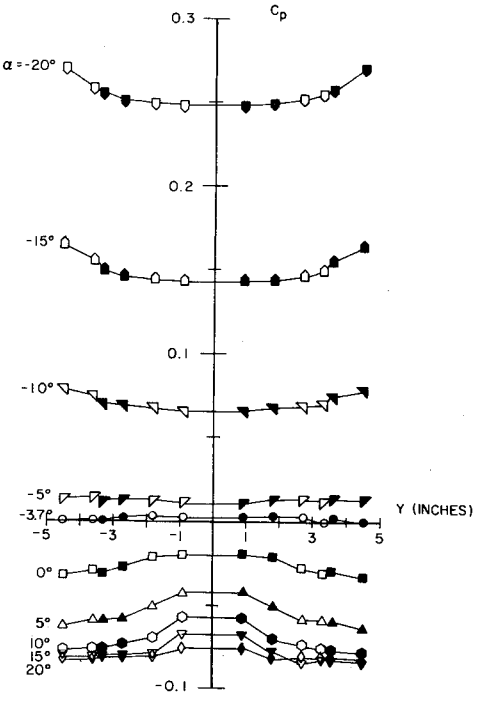

Fig. 6b Measured surface pressure coefficient on circular-cone waverider upper surface at various angles of attack ($M_\infty = 4$, $\beta = 0$, open symbols obtained by symmetry).

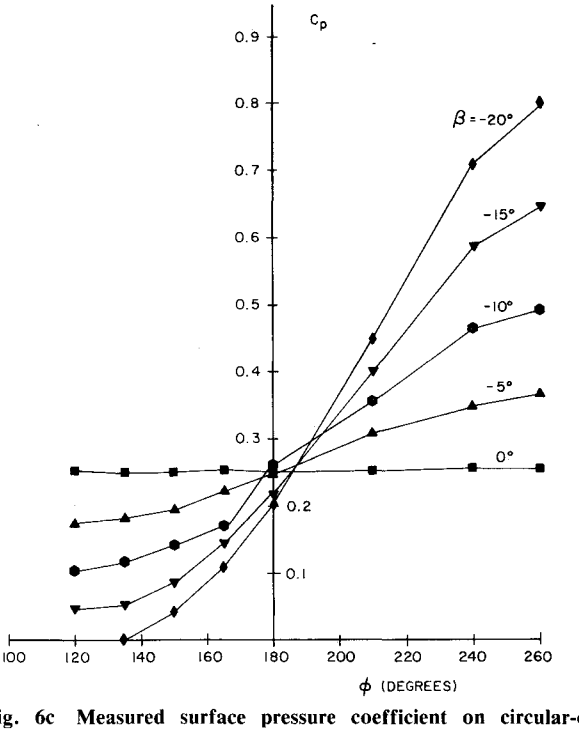

Fig. 6c Measured surface pressure coefficient on circular-cone waverider lower compression surface at various angles of yaw ($M_\infty = 4$, $\alpha = 0$).

of these waverider configurations were not conducted, there are no theoretical results in Fig. 6 for comparison. Numerical methods do exist, in principle, to calculate the off-design flowfield[11,12] although the calculations would be time-consuming and therefore expensive. In addition, the sharp leading edge of the waverider may present computational difficulties at extreme conditions when the shock wave is no longer attached.

Figure 7 gives analogous results for the surface pressure coefficient on the elliptic-cone waverider at $M_\infty = 4$. Again, the effects of Mach number variations in the range of 3-5 are small and thus results for $M_\infty = 3$ and 5 are not shown. In addition, these data do not show evidence of strong secondary shock waves for off-design conditions.

The data given in Figs. 6 and 7 show that as the angle of attack α is increased through positive values, the pressure coefficient on the windward symmetry line increases almost

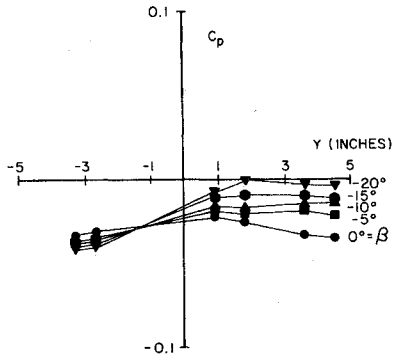

Fig. 6d Measured surface pressure coefficient on circular-cone waverider upper surface at various angles of yaw ($M_\infty = 4$, $\alpha = 0$).

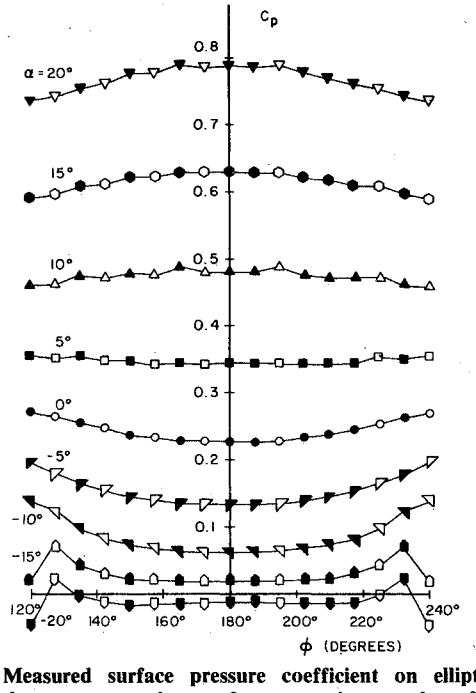

Fig. 7a Measured surface pressure coefficient on elliptic-cone waverider lower compression surface at various angles of attack ($M_\infty = 4$, $\beta = 0$, open symbols obtained by symmetry).

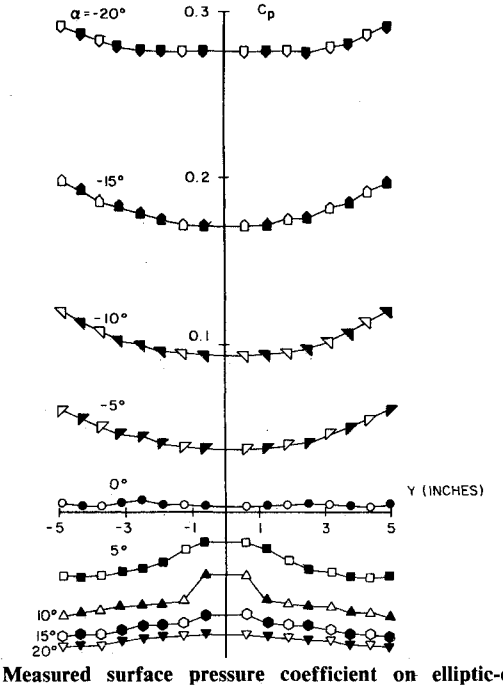

Fig. 7b Measured surface pressure coefficient on elliptic-cone waverider upper surface at various angles of attack ($M_\infty = 4$, $\beta = 0$, open symbols obtained by symmetry).

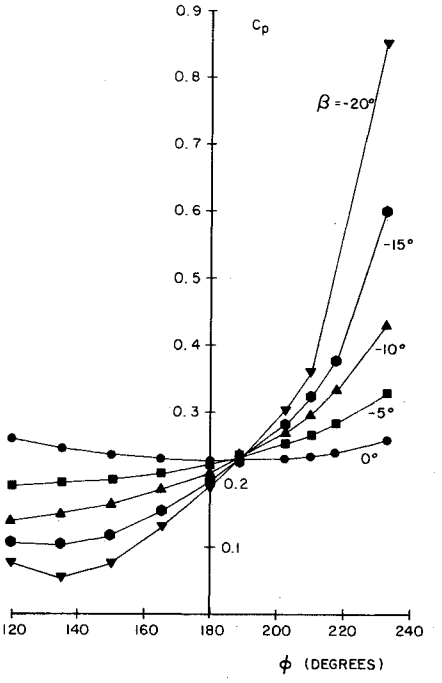

Fig. 7c Measured surface pressure coefficient on elliptic-cone waverider lower compression surface at various angles of yaw ($M_\infty = 4$, $\alpha = 0$).

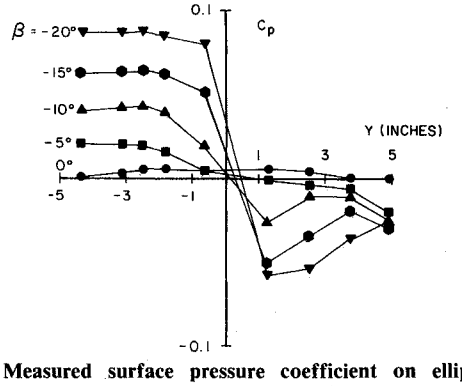

Fig. 7d Measured surface pressure coefficient on elliptic-cone waverider upper surface at various angles of yaw ($M_\infty = 4$, $\alpha = 0$).

linearly with α, while the pressure coefficient on the leeward surface decreases, again, almost linearly. Similarly, there is a nearly linear increase in the maximum surface pressure coefficient as the sideslip angle β increases.

Discussion and Conclusions

An extensive set of data for the surface pressure coefficient on two cone-derived waveriders has been presented along with comparative data for an elliptic cone. The waverider models are taken from a fundamental generic class of lifting bodies. The on-design conditions for these bodies is accurately described by the first-order perturbation theory of Rasmussen.[7] The data substantiate the accuracy of the theory for on-design conditions and show the deviations resulting from changes in both orientation and Mach number. The surface pressure data showed that the flow is always conical, without strong secondary shocks, over the entire range of conditions. These pressure data, when taken with earlier force and moment data and the associated theoretical analysis, enhance the case for these waverider bodies as attractive possibilities for furture hypersonic vehicle configurations.

Acknowledgments

This work was sponsored by the Air Force Armament Laboratory under Contract F08635-79-C-0017. The authors

gratefully acknowledge the help of Mr. Ronnie Broadaway in the preparation of this paper.

References

[1]Giragosian, P.A., "Critical Aerodynamic Technology Issues in Air-to-Air Missile Design," AIAA Paper 79-0089, New Orleans, La; Jan. 1979.

[2]Fleeman, E.L., "Aeromechanics Technologies for Tactical and Strategic Guided Missiles," presented at the AGARD FMP Meeting on Missile Systems Flight Mechanics, London, England, May 1979.

[3]Nielsen, J.N., "Missile Aerodynamics—Past, Present, Future," AIAA Paper 79-1819, New York, Aug. 1979.

[4]Doty, R.T. and Rasmussen, M.L., "Approximation for Hypersonic Flow Past and Inclined Cone," *AIAA Journal*, Vol. 11, Sept. 1973, pp. 1310-1315.

[5]Rasmussen, M.L. and Lee, H.M., "Approximation for Hypersonic Flow Past a Slender Elliptic Cone," AIAA Paper 79-0364, New Orleans, La., Jan. 1979.

[6]Jischke, M.C., "Supersonic Flow Past Conical Bodies with Nearly Circular Cross Sections," *AIAA Journal*, Vol. 19, Feb. 1981, pp. 242-245.

[7]Rasmussen, M.L., "Waverider Confirgurations Derived from Inclined Circular and Elliptic Cones," *Journal of Spacecraft and Rockets*, Vol. 17, Dec. 1980, pp. 537-545.

[8]Rasmussen, M.L., Jischke, M.C., and Daniel, D.C., "Experimental Forces and Moments on Cone-Derived Waveriders for $M_\infty = 3$ to 5, *Journal of Spacecraft and Rockets*, Vol. 19, Nov.-Dec. 1982, pp. 592-598.

[9]Pike, I., "Experimental Results from Three Cone-Flow Waveriders," AGARD Specialists Meeting, London, May 1968.

[10]Lanham, D.L., "Static Force, Pressure, and Oil-Flow Visualization Tests of Supersonic Aerodynamic Lifting Bodies at Mach Numbers 3 to 5," Arnold Engineering Development Center, Arnold Air Force Station, Tenn., AEDC TSR-80-VIZ, Feb. 1980.

[11]Siclari, M.J., "Investigation of Cross-Flow Shocks on Delta Wings in Supersonic Flow," *AIAA Journal*, Vol. 18, Jan. 1980, pp. 85-

[12]Kutler, P., "Computation of Three-Dimensional Inviscid Supersonic Flows,"*Progress in Numerical Fluid Dynamics, Lecture Notes in Physics*, Vol. 41, Springer-Verlag, Berlin, 1975, pp. 287-374.

[13]Jischke, M.C. and Rasmussen, M.L., "Aerodynamics of Supersonic Lifting Bodies," AFATL-TR-81-19, Feb. 1981.